ISSN: 3067-929X
Research Article

Journal of Electronics Science and Electrical Research

Trends in Metal-Insulator-Metal-Insulator- Metal Multilayers Built Using Fabry-Perot Cavities

Maria Masood*

Germany

***Corresponding author:** Maria Masood, Germany.

Submitted: 13 May 2025 **Accepted:** 19 May 2025 **Published:** 26 May 2025

https://doi.org/10.63620/MKJESER.2025.1010

Citation: *Masood, M. (2025). Trends in Metal-Insulator-Metal-Insulator- Metal Multilayers Built Using Fabry-Perot Cavities. J of Electron Sci and Electrical Res, 2(2), 01-20.*

Abstract

This chapter presents a comprehensive study on the design, analysis, and performance of Metal- Insulator-Metal-Insulator-Metal (MIMIM) multilayer stacks. The behavior of these stacks was modeled using the Transfer Matrix Method (TMM), allowing for a detailed investigation into their optical properties under varying parameters such as refractive index, layer thickness, polarization, and angle of incidence. The results highlight significant trends, including the effects of changing the incidence angle and layer thickness on reflection dips and absorption peaks, which exhibit wavelength-dependent shifts and intensity variations. These finding are particularly relevant for optimizing selective emitters in thermophotovoltaic (TPV) systems, where specific resonant peaks are desirable for efficient energy conversion. By adjusting the thickness of the metal and insulator layers, the study demonstrates how precise control over multilayer parameters can enhance performance, particularly through the strategic tuning of Fabry-Perot cavities within the stacks. The insights provided pave way for future applications in photonic and optoelectronic devices.

Keywords: Transfer Matrix Method, Multilayers, Thermophotovoltaics, Fabry-Perot Cavity

Introduction

In the pursuit of advancing our understanding of multilayer structures [1-4]. this research embarked on a comprehensive study of various multilayers, employing a range of materials and varying multiple parameters. The design and analysis of these multilayer stacks were carried out with a keen focus on optimizing the angle of incidence of incoming light, the thickness of each layer, the polarization and the refractive index. The parameters were adjusted systematically to explore their effects on the overall performance and behavior of multilayer structures.

This paper begins with a specific case study of a Metal-Insulator-Metal-Insulator-Metal (MIMIM) multilayer stack made of alternating TiN and Hafnia layers on a Si substrate. The choice of the materials and the MIMIM structure stem from their promising properties and potential application in various electronic and optical devices.

This study utilizes the Transfer Matrix Method (TMM) algorithm [5] to simulate the behavior of various multilayer stacks. TMM is a powerful computational technique used to model and predict the reflection, transmission and the absorption spectrum of multilayer stacks by solving Maxwell equations and computing the overall transfer matrix of the stack. Through these simulations a range of important results were uncovered. Various multilayers were studied exhaustively and some trends were noted in the optical response of these multilayers with a change in the refractive index, thickness of each layer, incidence angle and polarization. These findings provided valuable insights which helped massively while designing selective emitters for Thermophotovoltaic (TPV) systems. A good reference to understand the concept of TPV systems is [6].

In this research, a thorough analysis of the MIMIM stack is presented, discussing the specific parameters which were varied, and the resulting optical properties observed. This detailed in-

vestigation aims to highlight the complex interplay between the various factors that influence the behavior of multilayer stacks and to underline the importance of precise control over these parameters in the design of these stacks. The insights gained from this part of our research not only advance our theoretical understanding but also pave the way for practical applications in areas such as photonics and optoelectronics.

Description of the Multilayer Stack

The reference MIMIM multilayer stack studied in this paper is shown below in Table 1.

Table 1: The reference MIMIM stack.

Top Spacer Layer	Metal	Insulator	Metal	Insulator	Metal	Substrate
50nm Hafnia	20nm TiN	80nm Hafnia	20nm TiN	80nm Hafnia	20nm TiN	Si substrate

With reference to Table 1, there are alternating layers of metal and insulator on top of a thick Si substrate. The thickness of this substrate is considered large (in μm), so that the back reflections from the substrate into the multilayer can be neglected. The reference stack has considered similar thicknesses of the metal layers (20 nm), and also the two insulator layers sandwiched alternatively between the metal layers (80 nm). On top of this MIMIM stack is a dielectric spacer layer of 50 nm used to protect the MIMIM stack. A Metal-Insulator-Metal stack forms a well-known Fabry-Perot (FP) cavity. A good reference for understanding FP cavities are [7]. As shown in Error! Reference source not found., a FP cavity is two lossy metals, a distance apart, separated by a lossless dielectric. A FP cavity enhances the response of an optical system to radiation. The MIMIM multilayer stack in Table 1, therefore, has two tandem FP cavities, stacked on top of each other with a common metal layer. As will be investigated further, a minimum in the reflectance spectrum of the cavity is obtained as a consequence of the resonance of the cavity with the incident light wavelength. This reflectance spectrum (and by extension, the absorption spectrum by assuming negligible transmission) is obtained with the help of TMM simulations in python.

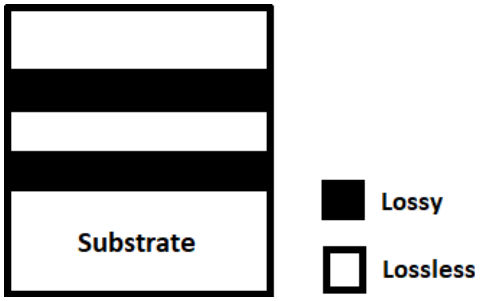

Figure 1: A Fabry-Perot Cavity.

The cavity is resonant with the incident light when the cavity field acquires a phase shift of the π order of m. 2, with respect to the incident light, where m is an integer.

If the reflectance of the FP cavity is considered, at resonance, the field reflected from the cavity is the superposition of the directly reflected input field and the cavity field that passes back π through the input metal layer. At resonance, there is a phase shift between the directly 2 reflected input field and the cavity field that passes back through the input metal layer. This causes destructive interference and as a result, there is a minimum in the reflection spectrum at the wavelength where there is resonance. This reflectance can be studied by obtaining the reflectance spectrum of the cavity by, for example, FTIR spectroscopy or theoretically, by TMM simulations. There is a way to also "predict" the resonance wavelength of a FP cavity at which the reflection is minimum. This was discussed in detail in [8] where phase analysis of a cavity was performed by Finite Difference Time Domain (FDTD) simulations.

Effect of Change of Angle of Incidence on Reflectance Dip of the Mimim Stack

The effect of changing angles of incidence on the reflection spectrum of the TiN/Hafnia multilayer was studied for different polarizations. A trend was observed in the changing position and intensity of the reflection dips. With increasing angle of incidence, these reflection dips shift to smaller wavelengths, because the component of the wave vector perpendicular to the layer surfaces decreases for a given wavelength, which is compensated by reducing the wavelength. This is also seen for 's' polarized and unpolarized incident light. 'p' polarized incident light For 'p' polarized light, an increase in the angle of incidence from 10 to 60° was studied for a Visible-NIR reflection spectrum of the TiN/Hafnia multilayer stack. As can be seen from the plots of Figure 2 and Figure 3, there were two prominent reflection dips and the intensity of the reflection curve, position and depth of the reflection dips varied with the angle of incidence. For 'p' polarized incident light, both the higher wavelength reflection dip and the lower wavelength reflection dip – within the range of 200nm to 1400nm – blue shift, almost linearly, as the angle of incidence increases from 10° to 80°.

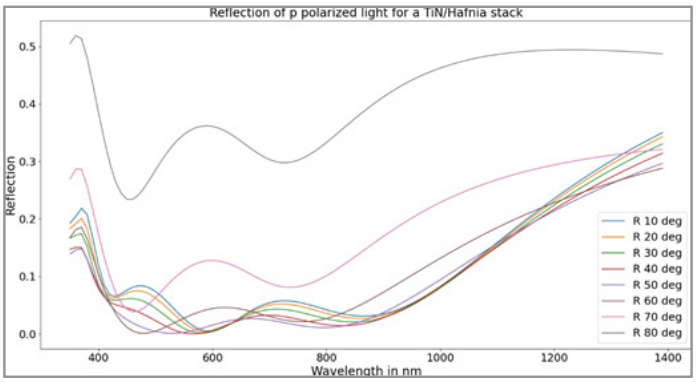

Figure 2: Reflection of 'p' polarized incident light for different angles of incidence for the MIMIM stack.

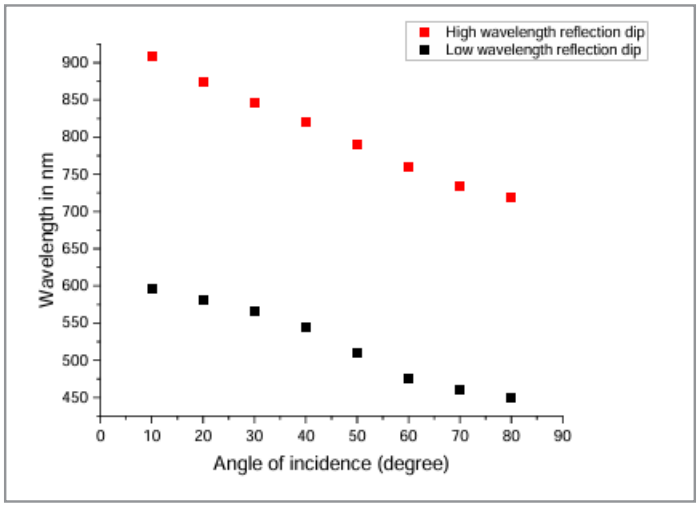

Figure 3: High wavelength and low wavelength reflection dip for different angles of incidence for 'p' polarized light.

The reflection spectrum of the TiN/Hafnia multilayer stack between 200 nm to 1400 nm range was studied for different angles of incidence for 's' polarized light. With reference to plots of Figure 4 and Figure 5, there were once again two reflection dips in the spectrum, and with increasing angles between 10 and 80°, both the reflection dips were blue shifted with respect to their wavelengths. It was also seen that the intensities of the reflection peaks greatly increase with an increase in the angle of incidence.

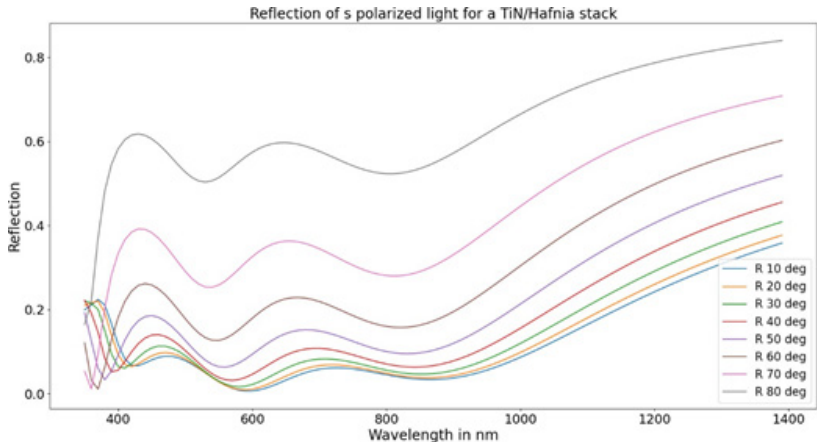

Figure 4: Reflection of 's' polarized incident light for different angles of incidence for the MIMIM stack.

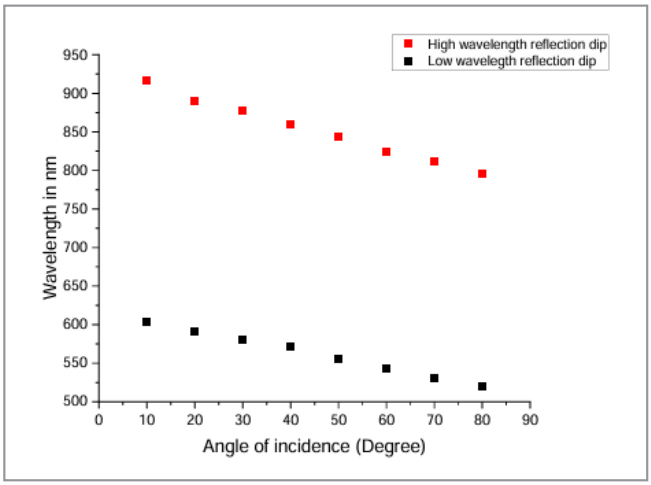

Figure 5: High wavelength and low wavelength reflection dip for different angles of incidence for 's' polarized light.

Unpolarized light The TiN/Hafnia multilayer stack was also studied for unpolarized light at different angles of incidence. Unpolarized light is light with random, time-varying polarization. It was interesting to note that the trend of the blue shift in the two reflection dips continued also for unpolarized impending light on the stack. As can be seen in the plots of Figure 6 and Figure 7, there was a clear blue shift in the wavelengths of the two reflection dips when the angle is increased from 60 to 80° with a step of 10°. Also, there was a definite increase in the intensities of the wavelength dependent reflection curves as the angle was increased from 10° to 80°.

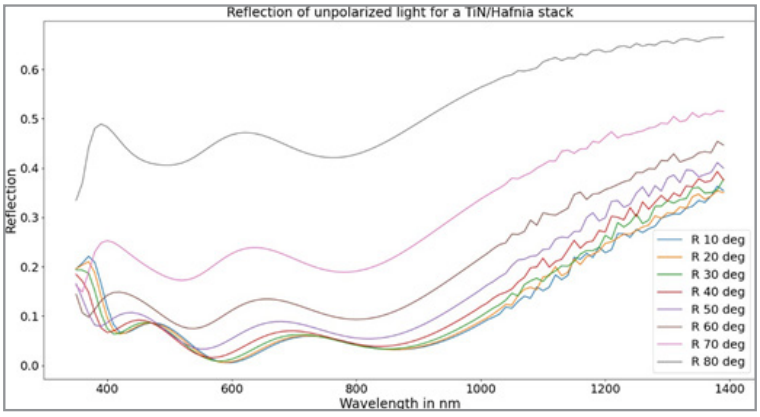

Figure 6: Reflection of unpolarized incident light for different angles of incidence for the MIMIM stack.

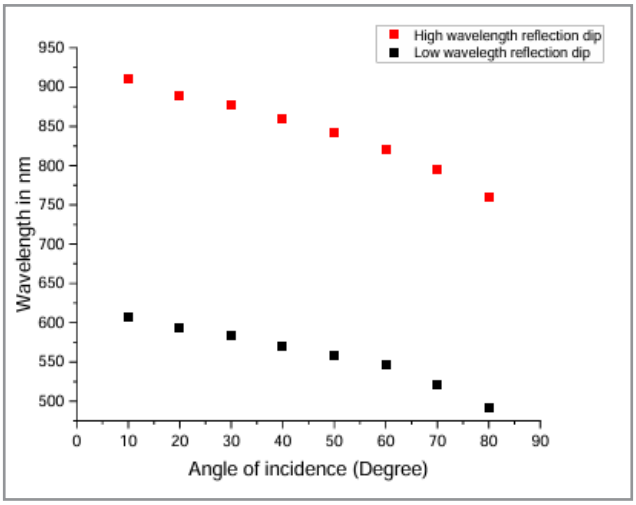

Figure 7: High wavelength and low wavelength reflection dip for different angles of incidence for unpolarized light.

Effects of Changing the Thickness of The Layers in The Stack

Changing the bottom metal layer

In this part of the simulations, the effect of changing the thickness of the bottom metal layer of the reference stack on the absorption spectrum of the reference MIMIM stack was studied. This is highlighted in the Table 2 below. The thickness of this layer was varied between 20 nm to 300 nm. As can be seen in Figure 8, there were two prominent peaks in the absorption spectrum.

Table 2: The bottom metal layer in the stack is varied.

Top Spacer Layer	Metal	Insulator	Metal	Insulator	Metal	Substrate
50nm Hafnia	20nm TiN	80nm Hafnia	20nm TiN	80nm Hafnia	20nm TiN	Si substrate

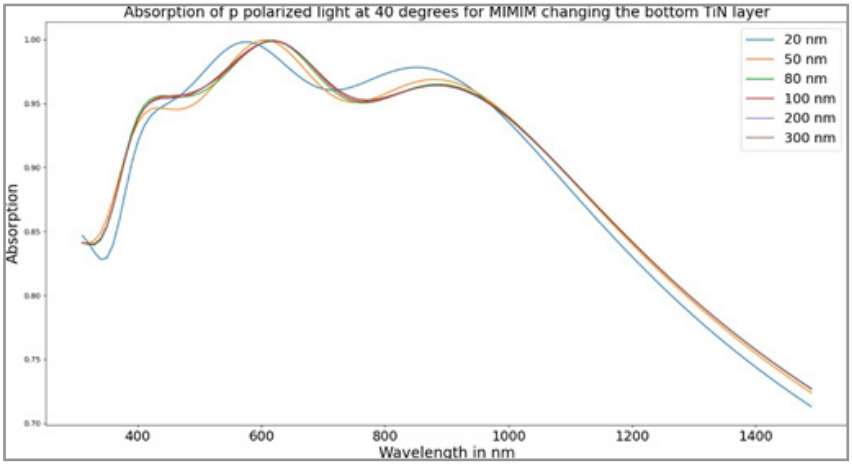

Figure 8: Absorption spectrum for reference spectrum, changing the bottom metal layer.

With reference to the plots of Figure 8 and Figure 9, as the thickness of the bottom metal layer just above the substrate was increased between 20 nm to 80 nm, the two prominent peaks shifted slightly to higher wavelengths. The intensity of the higher wavelength peak (Second peak) slightly decreased. For the lower wavelength peak (First peak), the intensity was the same. As the thickness is increased beyond 100 nm, the absorption spectrum was exactly the same.

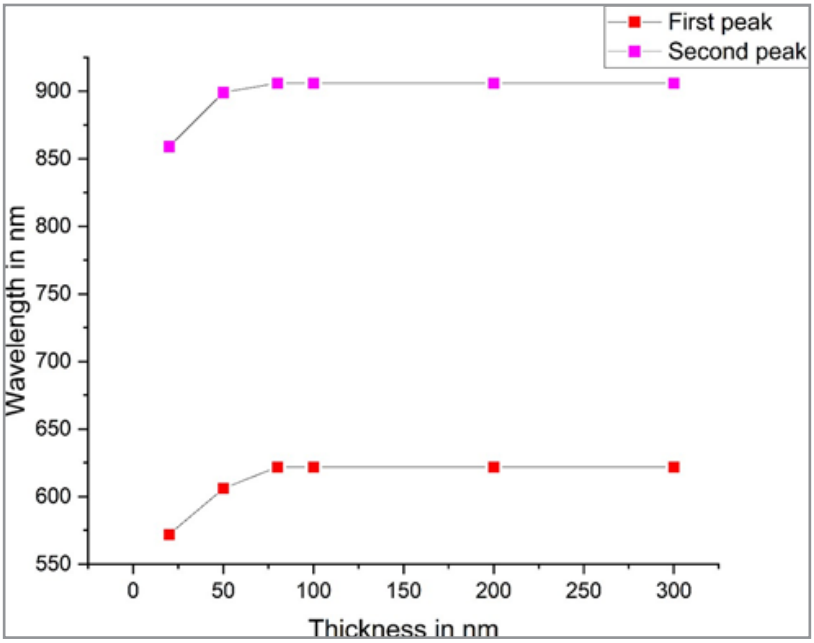

Figure 9: Peaks in absorption spectrum change with changing the bottom metal layer.

Changing the Insulator layer in the second cavity

The thickness of the insulator layer in the second cavity as shown in Table 3 was varied and the absorption spectrum of the stack with different thicknesses of this layer was compared.

There were two higher wavelength prominent peaks as seen in Figure 10. As is quantified in the Figure 11, the first peak shifted to higher wavelengths as the thickness of this insulator layer was increased. The second prominent peak however decreased in intensity as the thickness of this layer increased and disappeared for 170 nm and beyond. The absorption spectrum shifted to higher wavelengths as the thickness increased, and there were variations in the intensity and width of the peaks.

This was as expected for a Fabry-Perot Cavity, because as the thickness of the dielectric layer between the two metal layers is increased or decreased and the wavelength of the incident light remains the same, the resonant peak will not be at the same wavelength. This is because this produces the phase shift of the cavity, which changes the resonant wavelength. This was also seen when the dielectric layer in the top Fabry-Perot Cavity was changed.

Table 3: The insulator layer in the second cavity is varied.

Top Spacer Layer	Metal	Insulator	Metal	Insulator	Metal	Substrate
50nm Hafnia	20nm TiN	80nm	20nm TiN	80nm Hafnia	20nm TiN	Si substrate

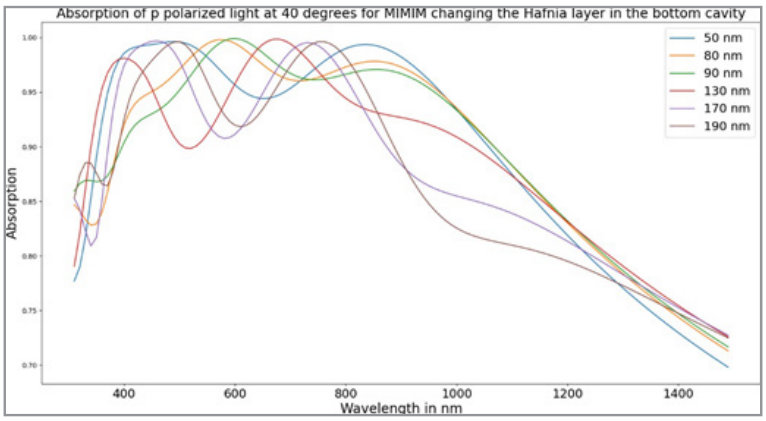

Figure 10: A comparison of absorption spectrum of the reference MIMIM stack, changing the insulator layer in the second cavity.

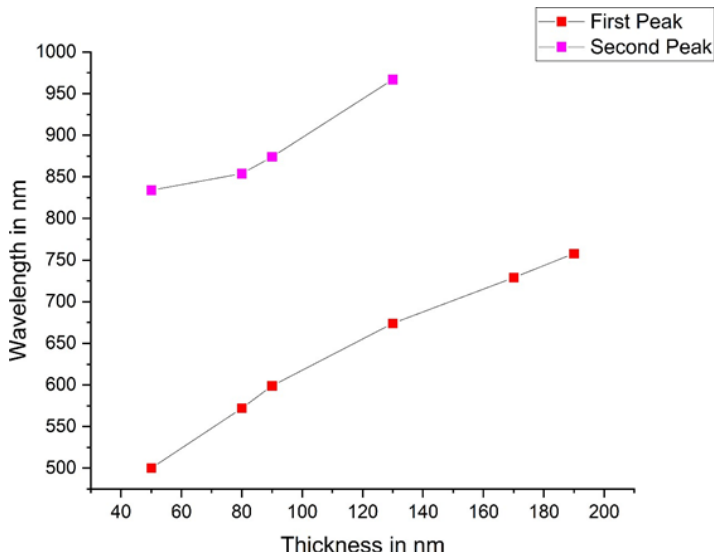

Figure 11: Peaks in the absorption spectrum change with changing the insulator layer in the second cavity.

Changing the Middle metal layer Thickness

A comparison of the absorption spectrums obtained by varying the thickness of the middle metal layer, as highlighted in Table 4, is shown in Figure 12.

Two prominent peaks were studied. The first prominent peak shifted to lower wavelengths, and the absorption spectrum was the same beyond 200nm thickness. When the thickness of the second peak was increased from 20 nm to 50 nm, the intensity of the peak decreased and the peak shifted slightly towards lower wavelengths. Beyond 50 nm, the second peak was the same.

Table 4: The middle metal layer is varied.

Top Spacer Layer	Metal	Insulator	Metal	Insulator	Metal	Substrate
50nm Hafnia	20nm TiN	80nm	20nm TiN	80nm Hafnia	20nm TiN	Si substrate

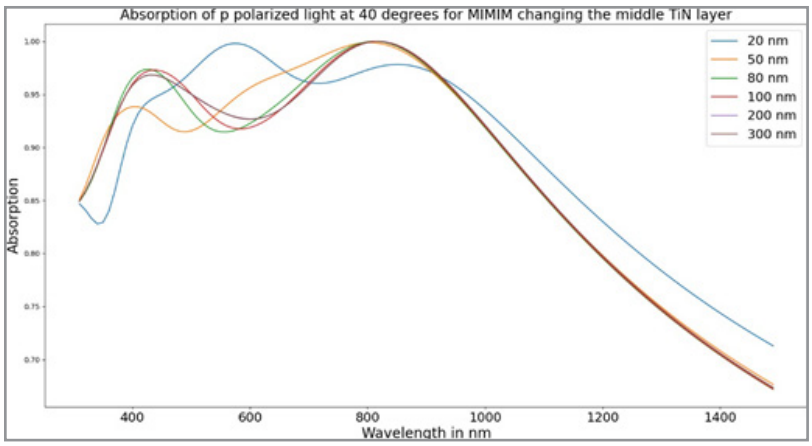

Figure 12: A comparison of absorption spectrum of the reference MIMIM stack, changing the middle metal layer.

Changing the insulator layer in the first cavity

As the insulator layer in the top Fabry-Perot Cavity (Table 5) was increased between 50 nm and 190 nm, the absorption peaks shifted to higher wavelengths. The intensity of the lower wavelength prominent peak (first peak) slightly decreased, but the decrease in the intensity of the higher wavelength prominent peak (second peak) was more pronounced. As mentioned before, this is an attribute of the phase change of the cavity with respect to the incident light. This can be seen in Figure 13 and Figure 14.

Table 5: The insulator layer in the first cavity is varied.

Top Spacer Layer	Metal	Insulator	Metal	Insulator	Metal	Substrate
50nm Hafnia	20nm TiN	80nm	20nm TiN	80nm Hafnia	20nm TiN	Si substrate

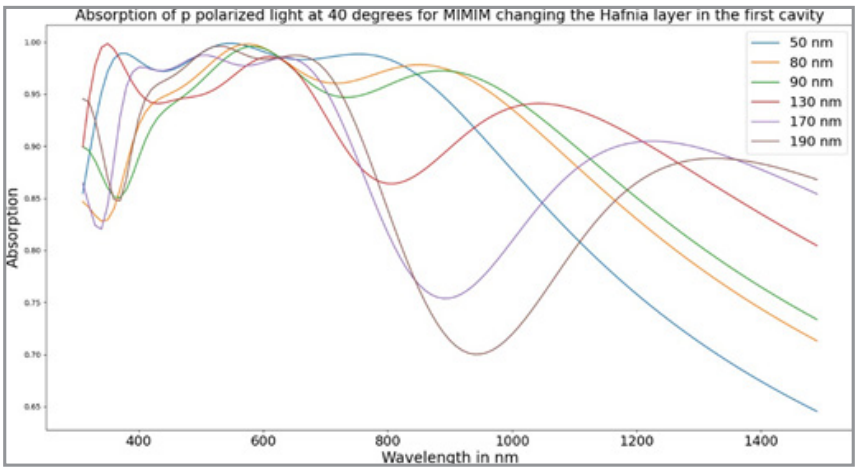

Figure 13: A comparison of absorption spectrum of the reference MIMIM stack, changing the insulator layer in the first cavity.

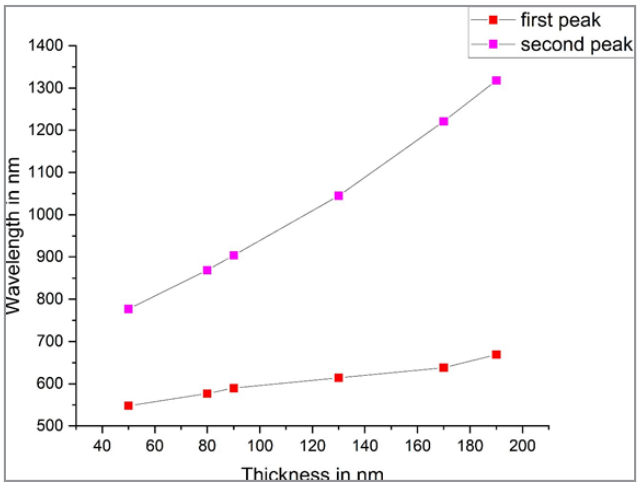

Figure 14: Peaks in the absorption spectrum shift with changing the insulator layer in the first cavity. Changing the first metal layer

Table 6: The first metal layer is varied.

Top Spacer Layer	Metal	Insulator	Metal	Insulator	Metal	Substrate
50nm Hafnia	20nm TiN	80nm	20nm TiN	80nm Hafnia	20nm TiN	Si substrate

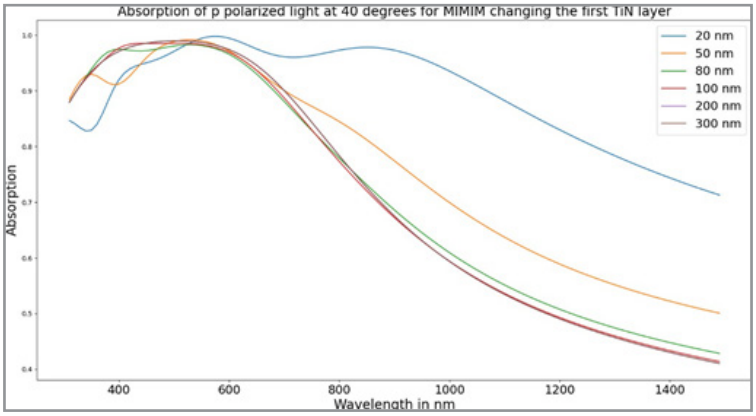

Figure 15: A comparison of absorption spectrum of the reference MIMIM stack, changing the top metal layer.

Changing the First Metal Layer Induced More Trends

The first metal layer thickness was studied in detail with reference to the second metal layer and the dielectric spacer layer thicknesses. The absorption of the reference stack at p polarized light at 40° angle of incidence with a thickness of 20 nm for the first metal layer was as shown in Figure 16. There were two prominent peaks in the absorption spectrum.

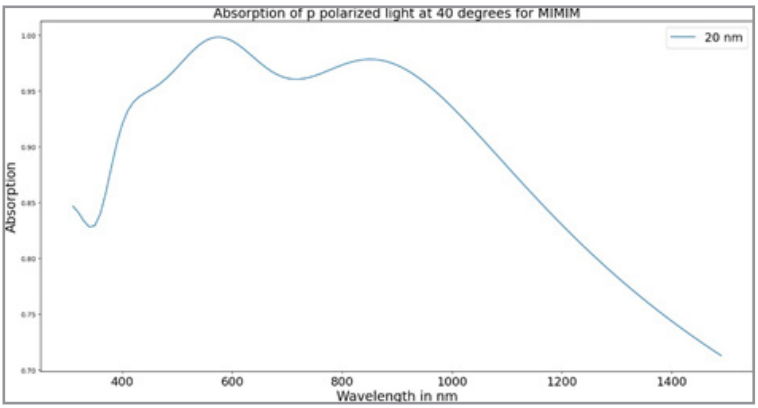

Figure 16: Absorption spectrum of the reference MIMIM stack (where the first metal layer is 20 nm).
The thickness of the first metal layer was changed as shown in the following Figure 17.

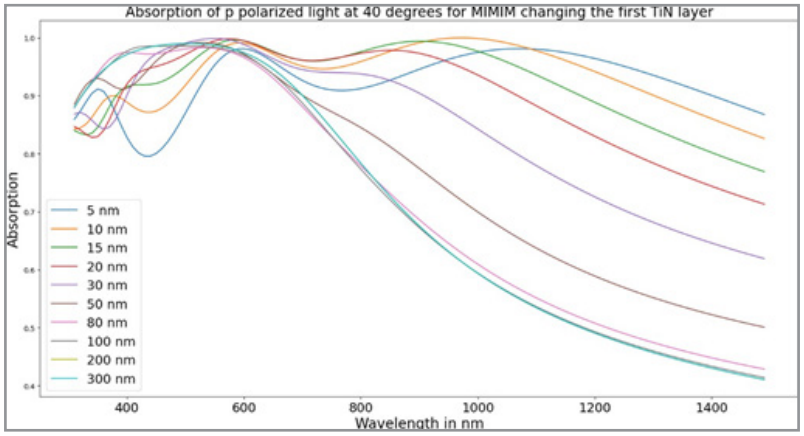

Figure 17: Absorption spectrums of the reference stack obtained on changing the thickness of the first metal layer.

In the top MIM cavity, it was noted, if the thickness of the top metal layer is greater than the thickness of the second metal layer, there were two prominent peaks in the absorption spectrum, as seen in the Figure 18 below.

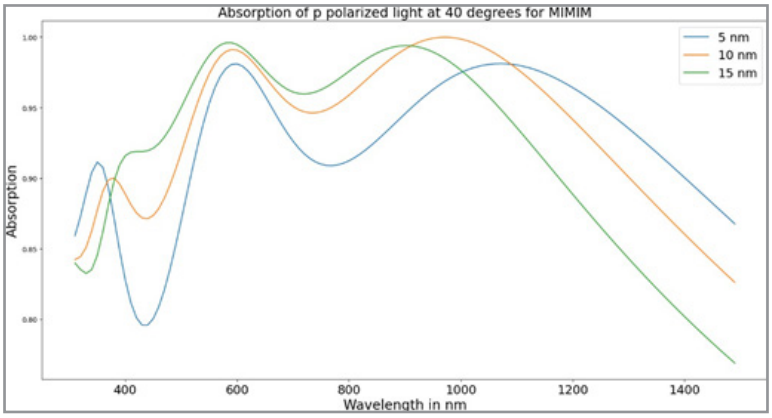

Figure 18: Thickness of the first metal layer is less than the thickness of the second metal layer. There are two prominent peaks in the absorption spectrum.

For a thicker top TiN layer in the first cavity, transmission through the first metal layer was significantly reduced. It was noted that the FP resonance of the second peak becomes weaker and the absorption intensity is reduced. The other prominent peak disappears eventually (Figure 19).

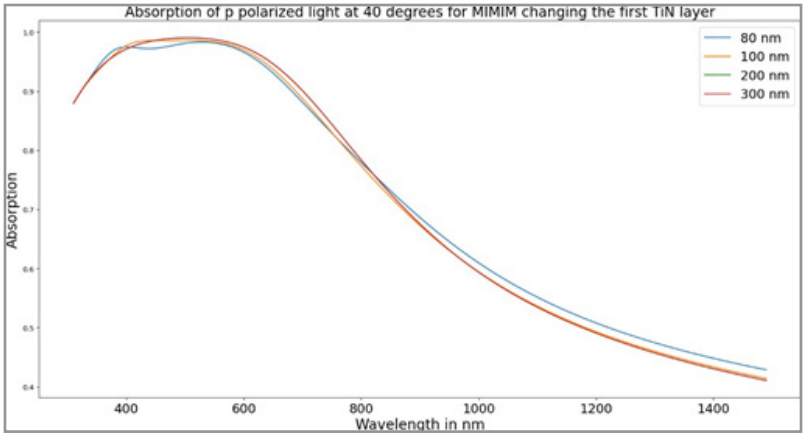

Figure 19: Thickness of the first metal layer is greater than the thickness of the second metal layer. There is only one prominent peak in the absorption spectrum.

When the dielectric coating thickness was greater than the thickness of the first metal layer another small peak was noticed at very low wavelength. To eliminate this small peak, the first metal layer was increased to beyond the dielectric coating thickness.

To see if this was valid, the dielectric coating thickness was increased to 80 nm, as an example. With reference to Figure 20 below, the dielectric coating in the reference stack was changed from 50 nm to 80 nm. Up to 80 nm thickness of the first metal layer, there was the small peak at the lower wavelengths. For the thickness of the first metal layer beyond 80 nm, the small peak disappears.

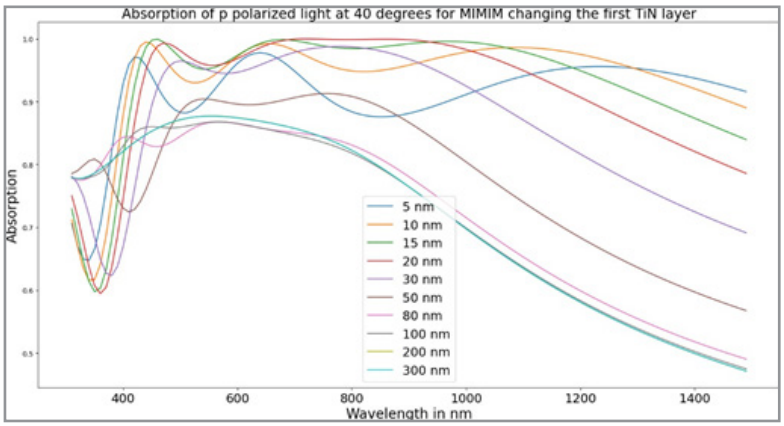

Figure 20: Absorption for MIMIM stack changing the first metal layer.

To check if this trend is also with MIMIM stacks with another metal, a MIMIM stack with Aluminum (Al) as the metal was studied as shown in Table 7.

Table 7: MIMIM stack with another metal, Aluminum (Al).

Top Spacer Layer	Metal	Insulator	Metal	Insulator	Metal	Substrate
50nm Hafnia	20nm TiN	80nm	20nm TiN	80nm Hafnia	20nm TiN	Si substrate

Many simulations were done to check this, and it was realized that the above trend for the top FP cavity of the MIMIM stack continued also for this stack. This is shown in Figure 21.

There were two peaks in the absorption spectrum of Table 7. When the thickness of the first metal layer was increased beyond the thickness of the second metal layer (of 50 nm), one of the peaks was suppressed entirely, and there was no change in the spectrum beyond a certain thickness.

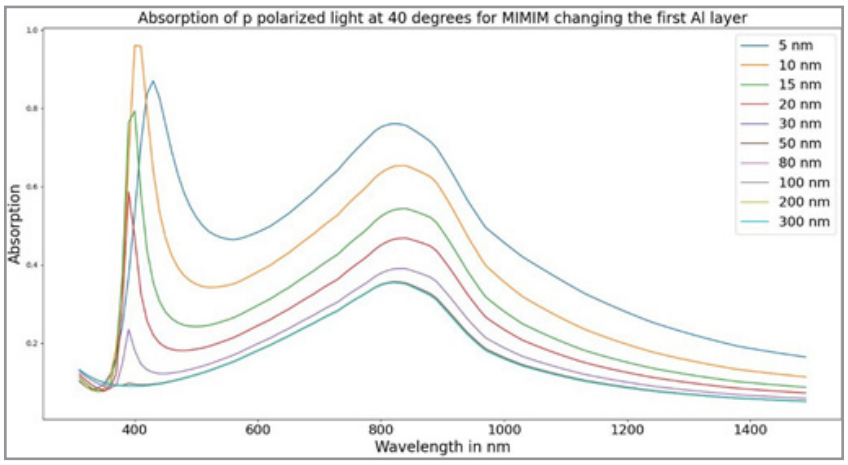

Figure 21: Same trend observed in another multilayer stack with Aluminum as the metal. One of the prominent peaks is completely suppressed when the thickness of the first metal layer is greater than that of the second metal layer.

Changing the Source of Refractive Index

The refractive index for TiN for all the above simulations in sections 2, 3 and 4 were obtained by ellipsometry measurements of a wafer which was a simple 100 nm TiN layer on Si substrate. The refractive index of the Si substrate was taken as 3.97 for n and 0.03 for k.

To explore what happens when the n and k values are obtained from another source, measurements were done for refractive index of TiN obtained from the parameters from RefFIT fit of another wafer. The n and k for Si substrate was taken from the database and the change in these values with respect to the wavelength was also considered.

Thereby, the following plots were obtained, and there were variations in the absorption spectrum of the stack. The blue plots are for the n and k of TiN obtained with the ellipsometry measurements, and a constant n and k for Si. The black plots are for the n and k of TiN obtained from the RefFIT fit and n and k of Si varying with respect to the wavelength.

The main purpose of this section was to show that there are variations in the simulated absorption spectrums when the refractive index is changed and the n and k of the Si substrate are considered varying with the wavelength, and hence each plot is not compared separately. Figure 22 to Figure 26.

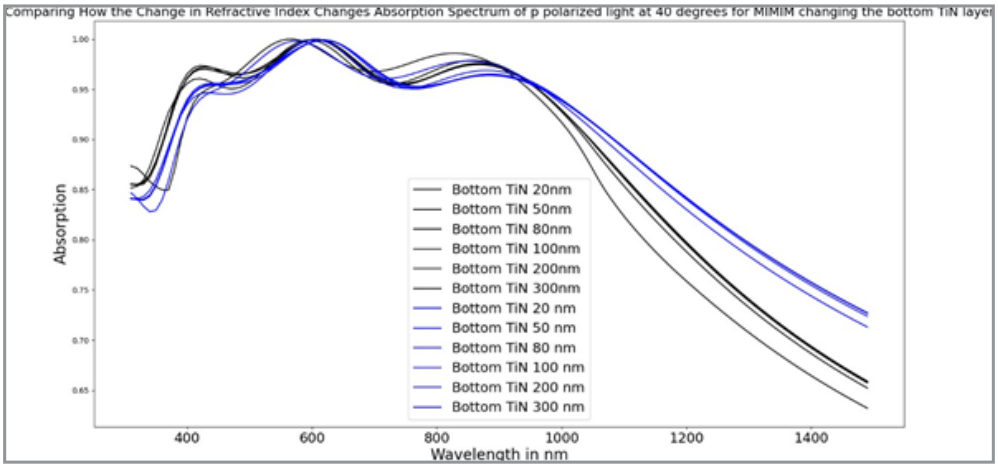

Figure 22: Absorption spectrum changing the bottom metal layer with refractive index from different sources. There is a change in the absorption spectrum. The blue plots are for the n and k of TiN obtained with the ellipsometry measurements, and a constant n and k for Si. The black plots are for the n and k of TiN obtained from the RefFIT fit and n and k of Si varying with respect to the wavelength.

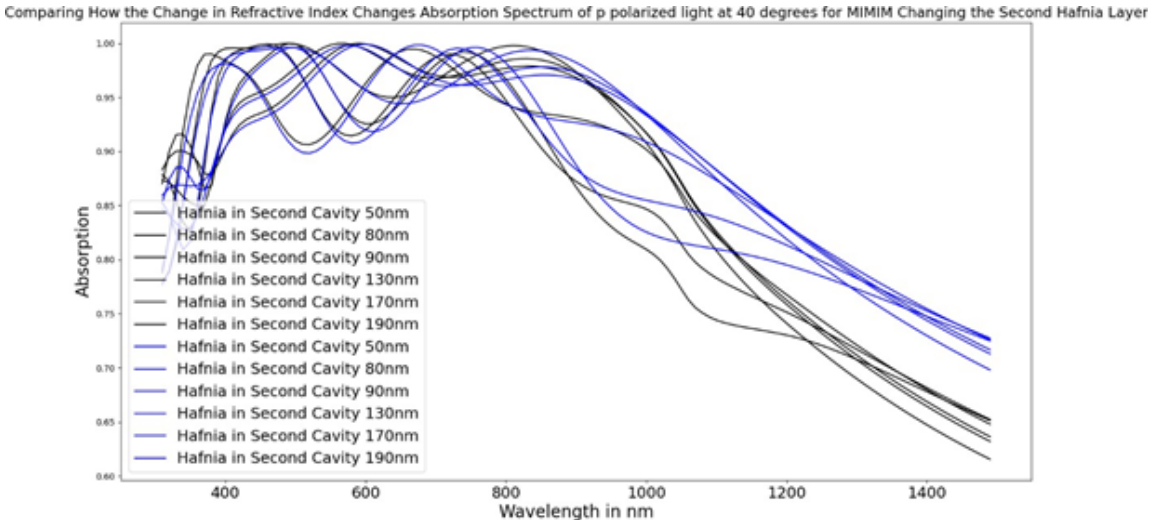

Figure 23: Absorption spectrum changing the insulator layer in the second cavity with refractive index from different sources. There is a change in the absorption spectrum. The blue plots are for the n and k of TiN obtained with the ellipsometry measurements, and a constant n and k for Si.

The black plots are for the n and k of TiN obtained from the RefFIT fit and n and k of Si varying with respect to the wavelength.

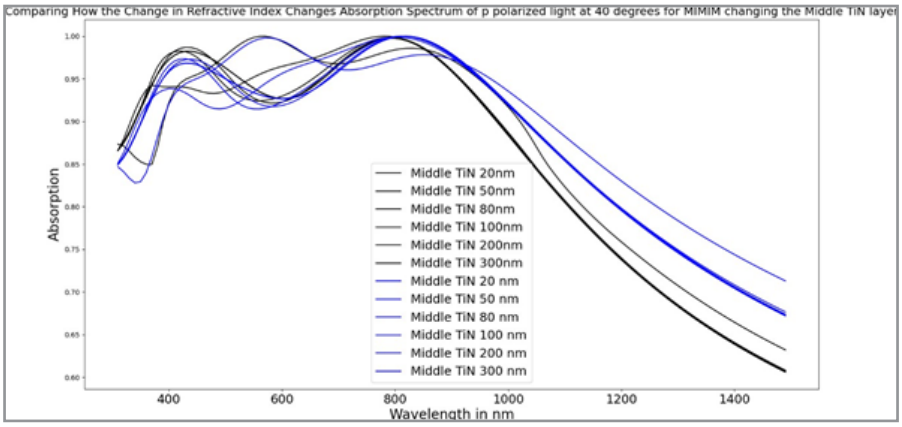

Figure 24: Absorption spectrum changing the middle metal layer with refractive index from different sources. There is a change in the absorption spectrum. The blue plots are for the n and k of TiN obtained with the ellipsometry measurements, and a constant n and k for Si. The black plots are for the n and k of TiN obtained from the RefFIT fit and n and k of Si varying with respect to the wavelength.

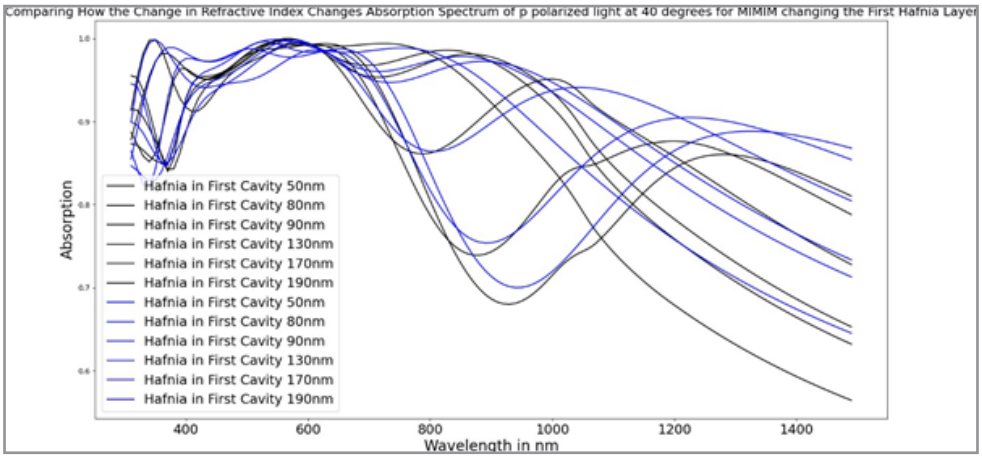

Figure 25: Absorption spectrum changing the insulator layer in the first cavity with refractive index from different sources. There is a change in the absorption spectrum. The blue plots are for the n and k of TiN obtained with the ellipsometry measurements, and a constant n and k for Si.

The black plots are for the n and k of TiN obtained from the RefFIT fit and n and k of Si varying with respect to the wavelength.

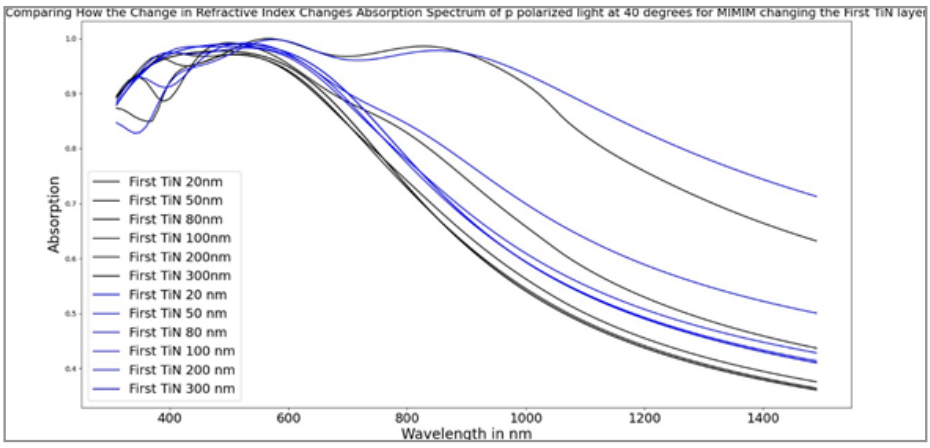

Figure 26: Absorption spectrum changing the first metal layer with refractive index from different sources. There is a change in the absorption spectrum. The blue plots are for the n and k of TiN obtained with the ellipsometry measurements, and a constant n and k for Si. The black plots are for the n and k of TiN obtained from the RefFIT fit and n and k of Si varying with respect to the wavelength.

Absorption V/S Depth

To check how each layer contributes to the absorption in the stack at a particular wavelength, the absorption versus depth profile of the reference stack presented earlier is as shown in Figure 27. As an example, five wavelengths were studied and for example, at 1075 nm wavelength of incident radiation, there was zero absorption in the dielectric layer (as would be the case), and the maximum absorption was in the top metal layer. In the second dielectric hafnia layer, there was zero absorption. Deeper in the second metal layer from the top, there was absorption, and the trend continued up to the depth of the Si substrate.

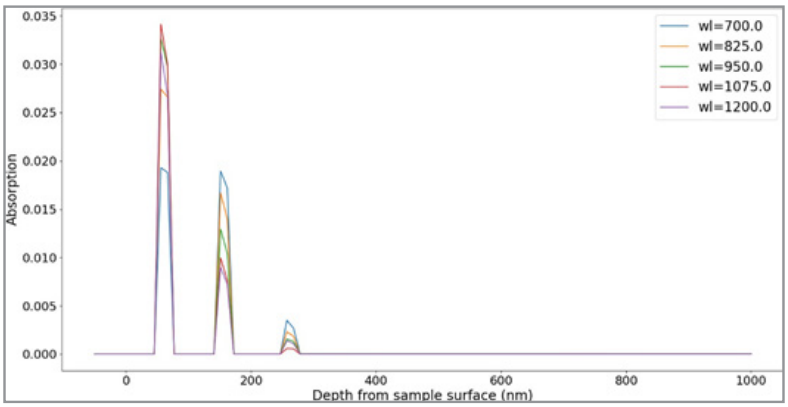

Figure 27: Absorption vs depth profile of the reference MIMIM multilayer stack.

To understand this better, the absorption was studied layer-by-layer for another simple multilayer stack with one FP cavity as shown in Table 8 and figures that follow (Figure 28, Figure 29, Figure 30, Figure 31 and Figure 32). With reference to the absorption vs depth profile of this stack, the absorption is only in the metal layers and the absorption in the dielectric layers is zero. It can be inferred that the metal layers of the FP cavity act as reflectors of light, and the dielectric layer inside is the lossless layer. At any wavelength of incident radiation, the total absorption sums up to 100%.

Table 8: A simpler MIM FP cavity multilayer stack to study the absorption in each layer.

Top Spacer Layer	Metal	Insulator	Metal	Substrate
90nm Hafnia	40nm TiN	195nm Hafnia	400nm TiN	Si substrate

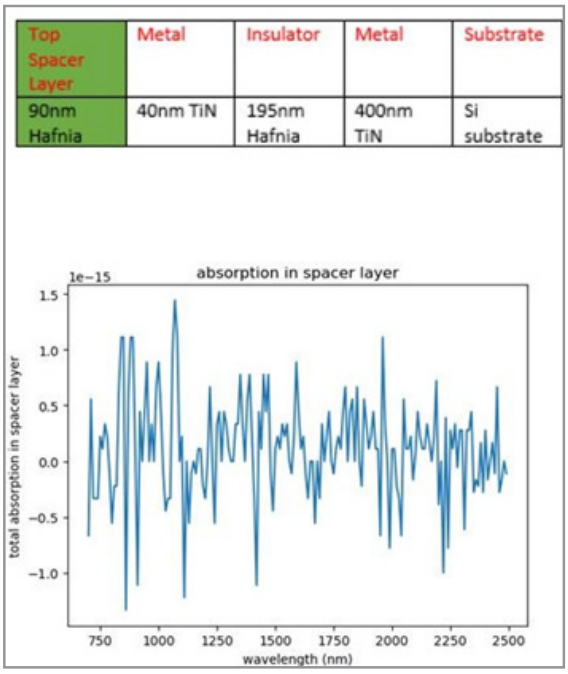

Figure 28: Study of absorption in each layer: Absorption in the top dielectric spacer layer.

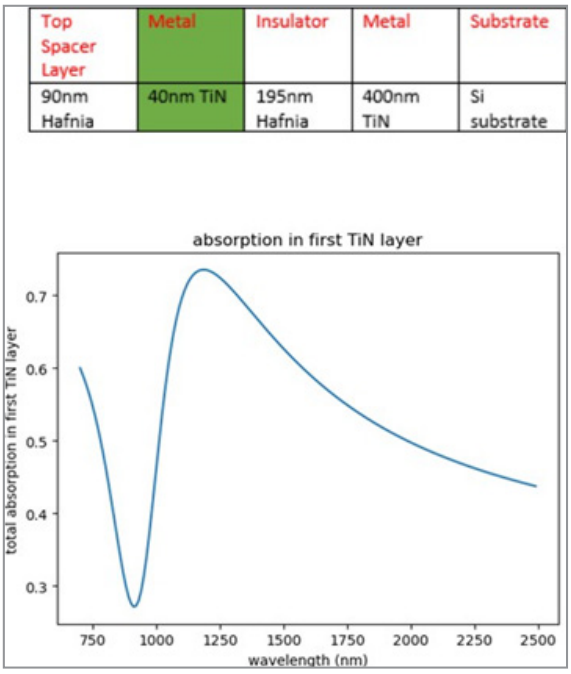

Figure 29: Study of absorption in each layer: Absorption in the top metal layer.

Top Spacer Layer	Metal	Insulator	Metal	Substrate
90nm Hafnia	40nm TiN	195nm Hafnia	400nm TiN	Si substrate

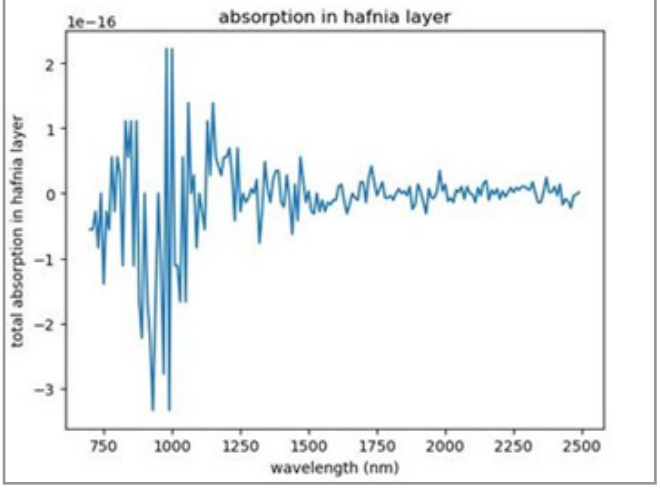

Figure 30: Study of absorption in each layer: Absorption in the middle dielectric layer.

Top Spacer Layer	Metal	Insulator	Metal	Substrate
90nm Hafnia	40nm TiN	195nm Hafnia	400nm TiN	Si substrate

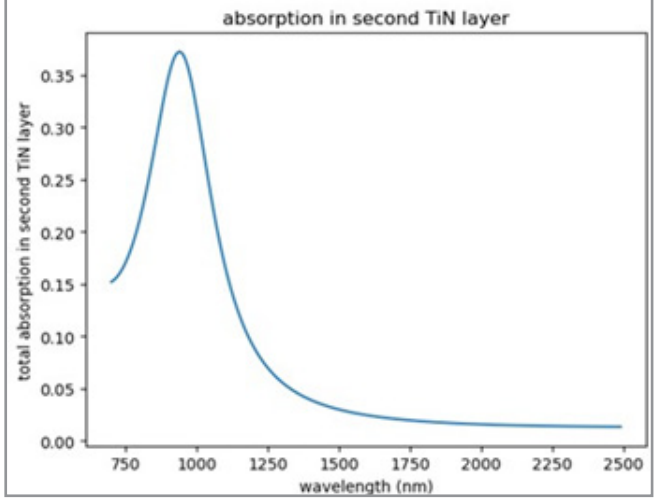

Figure 31: Study of absorption in each layer: Absorption in the bottom metal layer.

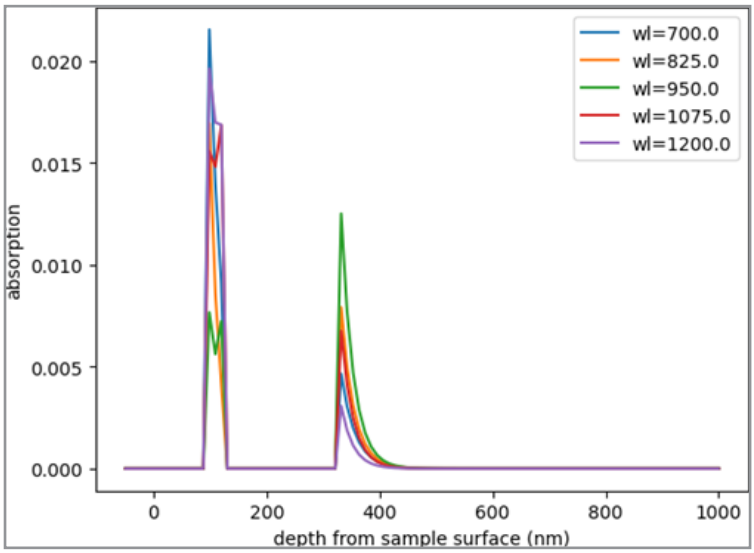

Figure 32: Absorption vs depth profile of the simpler MIM multilayer stack of Table 8.

R, T and A by Changing Different Parameters at Once

Effect of Changing the Thickness of Different Layers (Also Simultaneously Changing the Angle of Incidence and Wavelength)

XYZPY is a library in python used for, among other tasks, efficiently plotting data which has a lot of dimensions [9]. In this section, the reflection, transmission or absorption of a multilayer stack are plotted against the thickness of each layer, angle of incidence and wavelength in one plot.

Reflectance

The density plots of the reflectance of the stack created using the XYZPY library are as shown in Figure 33. It was easy to create these plots using code, and these plots with more dimensions of data can be easily interpreted. Using these plots, it is easy to find the combination of the angle of incidence and thickness of the layers to obtain the desired reflectance at any wavelength between 500 nm and 2000 nm. For example, with reference to Figure 33 (a), when the thickness of the top TiN metal layer was

kept at 100 nm and the angle of incidence between 0 and 40°, a high reflectance peak can be achieved between 1000 nm and 2000 nm wavelength.

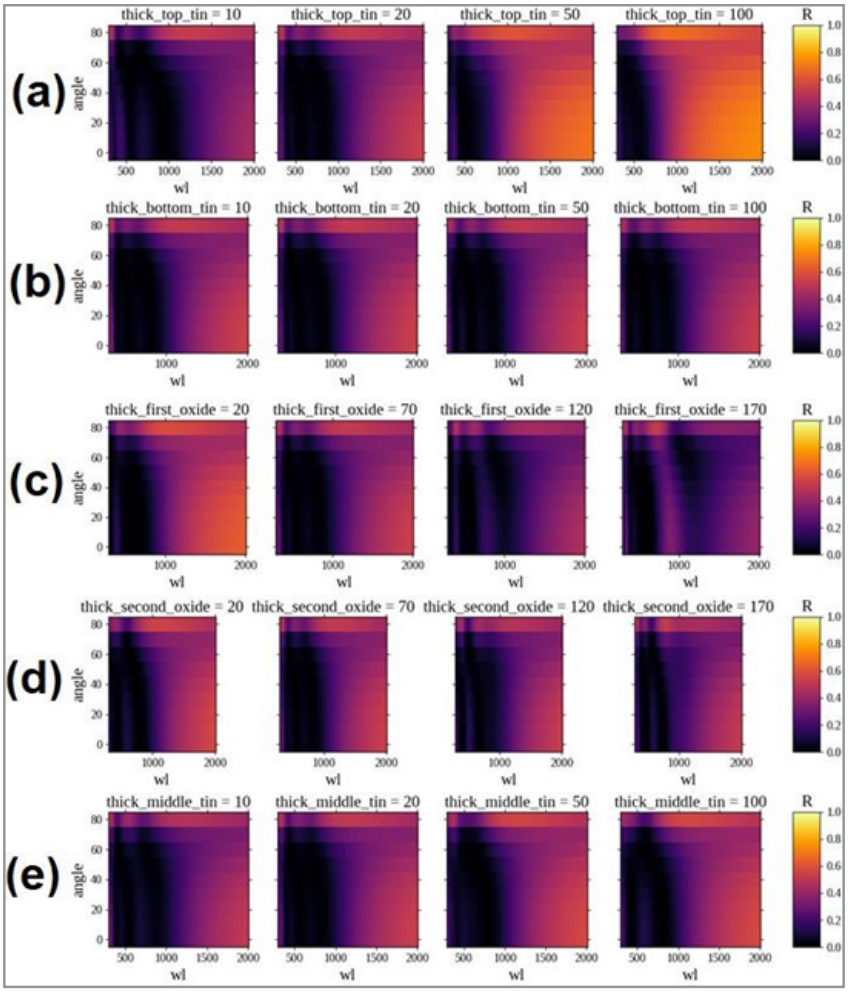

Figure 33: XYZPY plots of reflectance of a multilayer stack with changing angle of incidence. Changing the thickness of (a) top TiN metal layer (b) bottom TiN metal layer (c) top dielectric spacer layer (d) second dielectric layer (e) middle TiN metal layer.

Transmittance

The density plots from Figure 34 for the Transmittance of the reference stack show that there was no transmittance across the stack no matter what the thickness, angle of incidence or wavelength.

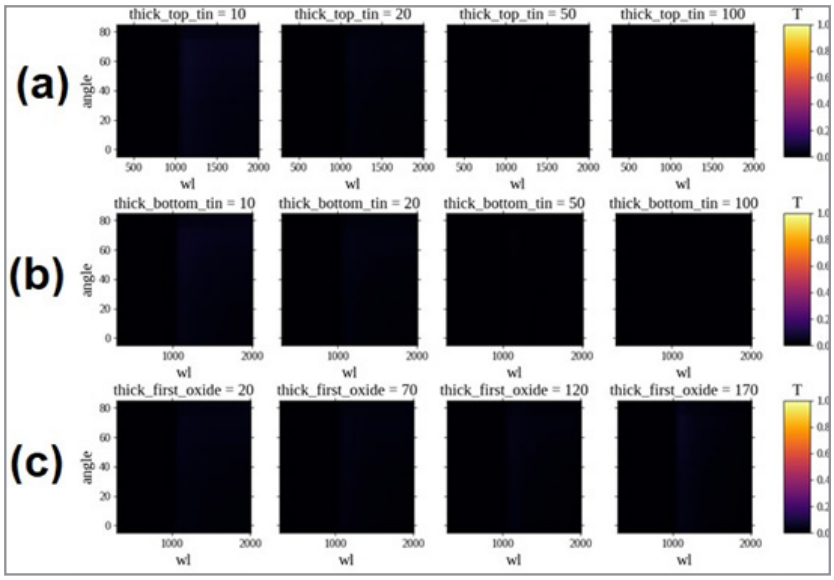

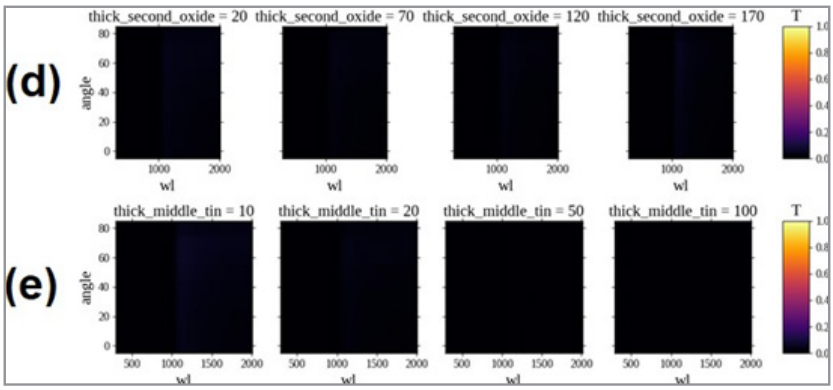

Figure 34: XYZPY plots of transmittance of a multilayer stack with changing angle of incidence. Changing the thickness of (a) top TiN metal layer (b) bottom TiN metal layer (c) top dielectric spacer layer (d) second dielectric layer (e) middle TiN metal layer.

Absorption

The main objective of this research was to create a multilayer stack which has high absorption around a desired wavelength range. During the design of these multilayers for applications as selective emitters, XYZPY plots proved to be very efficient in predicting the amount of absorption at a particular wavelength given the thickness of each layer and angle of incidence, and the need to repeat all TMM stimulations to try all the combinations one by one which would be extremely time consuming was eluded. The absorption XYZPY plots of the reference multilayer stack in Table 1 is shown in Figure 35 for different thicknesses and angles of incidence.

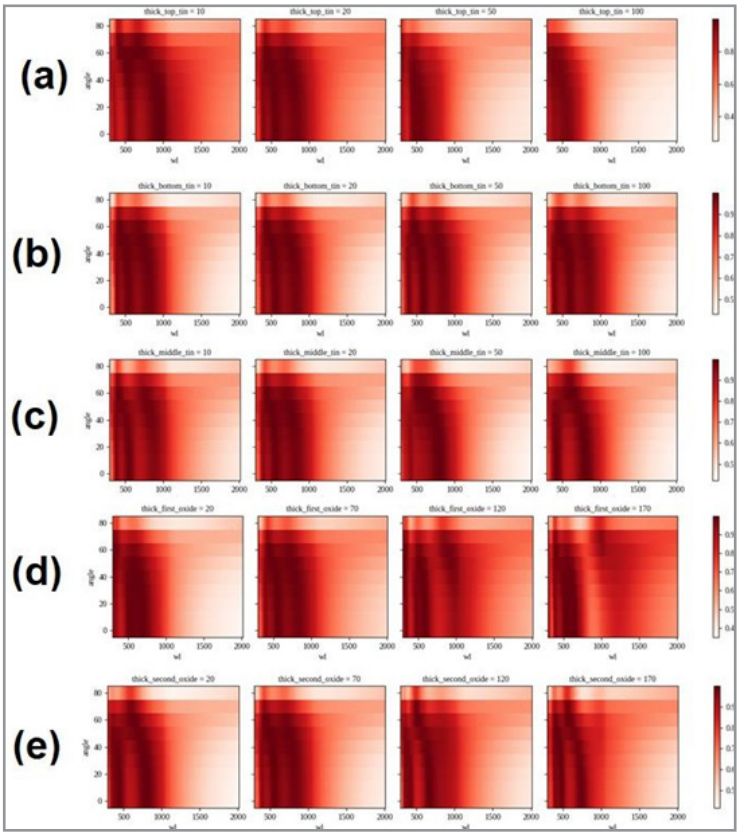

Figure 35: XYZPY plots of absorption of a multilayer stack with changing angle of incidence.

Same Trend Observed in Another Multilayer Stack

Another MIM cavity was studied to see if the trends in the effect of change of angle of incidence and polarization on the reflection spectrum remains. This cavity was made of alternating Al/Hafnia layers on top of a Si substrate. A 400 nm Al metal layer on top of the substrate, on which there is a 425 nm dielectric Hafnia layer, followed by another very thin layer of 10 nm Al metal on top, and a top dielectric spacer layer of 90nm Hafnia. This multilayer stack is shown in Table 9.

Table 9: Another MIM multilayer stack to study if the trend remains.

Top Spacer Layer	Metal	Insulator	Metal	Substrate
90nm Hafnia	10nm Al	425nm Hafnia	400nm Al	Si substrate

This section reports the effect of change of angle of incidence on reflectance dip of the MIM stack in Table 9 for:

- 'p' polarized incidence light
- 's' polarized incidence light
- unpolarized incidence light

In general, much deeper reflectance dips in this stack of Al/Hafnia multilayers were seen, because of the higher absorption coefficient of Al compared to TiN, this was studied in detail in [10].

'p' Polarized Incident Light

The two prominent dips in the reflectance spectra of the MIM stack of Table 9 shift to lower wavelengths as the angle of incidence was increased from 0 to 90°. This is the same trend as observed in the MIMIM stack of TiN and Silica nano layers on Si substrate in Table 1. The higher wavelength reflection dip was slightly deeper as the angle of incidence increases. On the other hand, the lower wavelength reflection dip decreased as the angle of incidence was increased. As reported in the previous sections, the reflectance dip at very low wavelengths was due to the top metal layer being thinner than the dielectric coating layer.

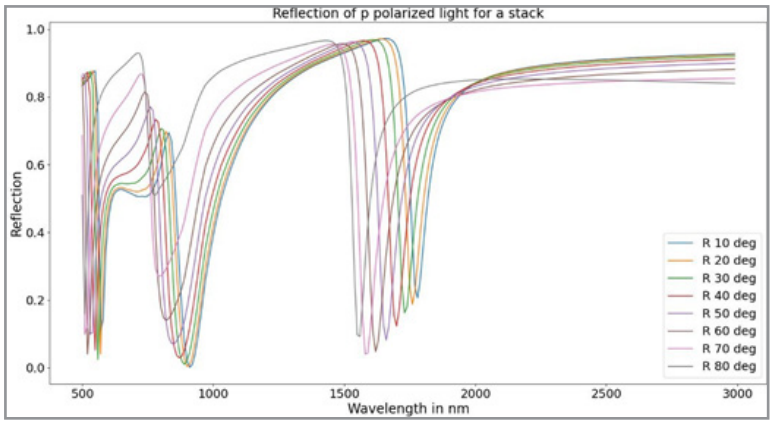

Figure 36: Reflectance spectrum of MIM stack of Al/Hafnia multilayer stacks for 'p' polarized light showing the same trend as the MIMIM stack.

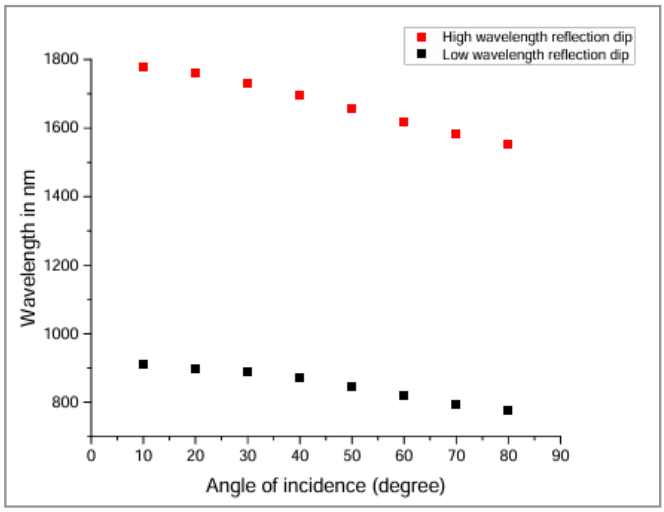

Figure 36: Reflectance spectrum of MIM stack of Al/Hafnia multilayer stacks for 'p' polarized light showing the same trend as the MIMIM stack.

For the ′s′ polarized incidence light, as the angle of incidence was increased, both the prominent reflection dips in the reflectance spectra shifted to lower wavelengths. The higher wavelength reflection dip decreased and so did the lower wavelength reflection dip. This was also noted as a trend. The reflectance dip at very low wavelengths is due to the top metal layer being thinner than the dielectric coating layer.

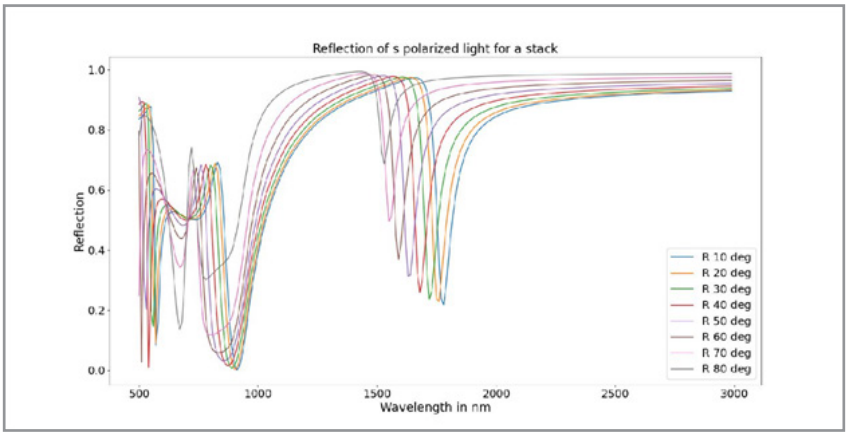

Figure 38: Reflectance spectrum of MIM stack of Al/Hafnia multilayer stacks for 's' polarized light showing the same trend as the MIMIM stack.

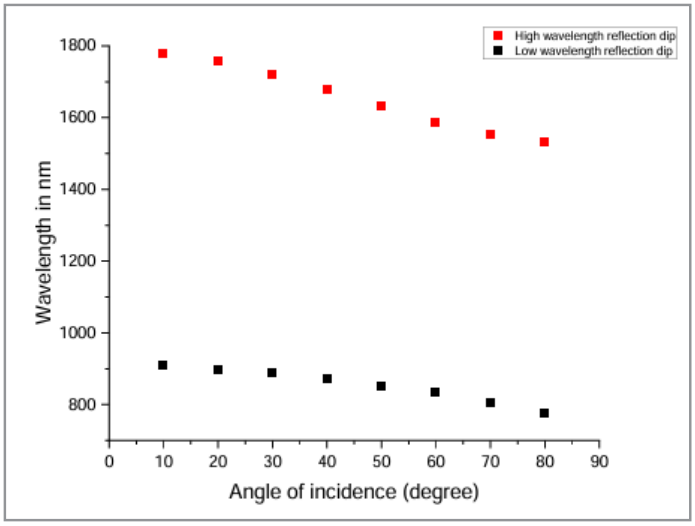

Figure 39: High wavelength and low wavelength reflection dip for different angle of incidence for 's' polarized light unpolarized incident light

Both the prominent higher wavelength reflection dip and lower wavelength reflection dip decreased and shifted to lower wavelengths as the angle of incidence was increased, for unpolarized light too. The reflectance dip at very low wavelengths was due to the top metal layer being thinner than the dielectric coating layer.

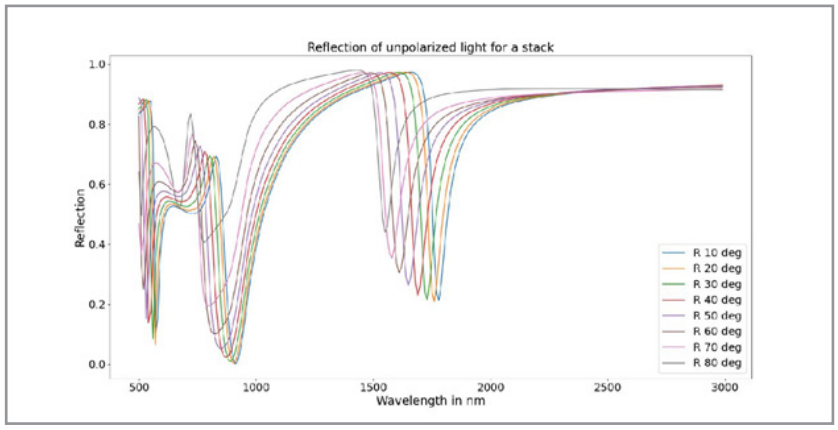

Figure 40: Reflectance spectrum of MIM stack of Al/Hafnia multilayer stacks for unpolarized light showing the same trend as the MIMIM stack.

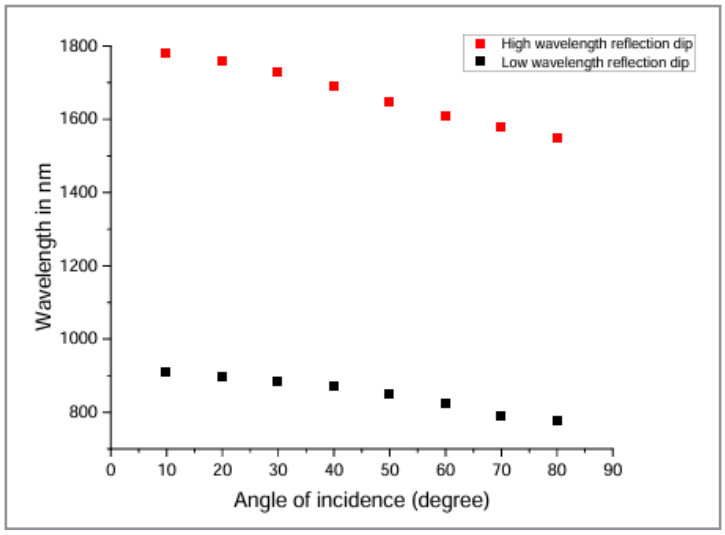

Figure 41: High wavelength and low wavelength reflection dip for different angle of incidence for unpolarized light.

It is beneficial to mention here that in this stack also, there were two main reflection dips in the reflection spectrum, because the top metal layer thickness was less than that of the bottom metal layer, and hence there were two main peaks in absorption (two reflection dips). To cross-check this statement also, a quick set of simulations were run for stack with the top metal layer thickness increased to be more than the bottom metal layer thickness (from 10nm to 420nm), and it was noted that there is now only one reflection dip, as shown in the plots in Figure 42.

Table 10: The first metal layer thickness is increased to be greater than the second metal layer thickness.

Top Spacer Layer	Metal	Insulator	Metal	Substrate
90nm Hafnia	420nm Al	425nm Hafnia	400nm Al	Si substrate

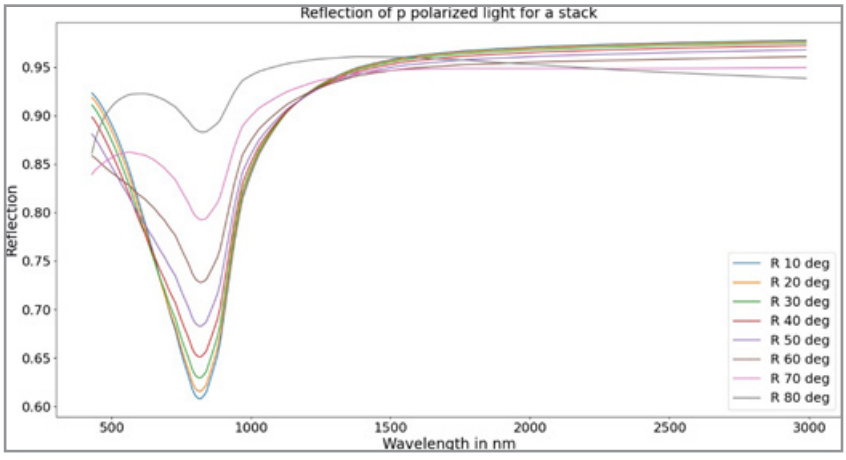

Figure 42: Making the top metal layer thickness greater than the second metal layer thickness results in only one prominent reflection dip (and hence, absorption peak), for all angles of incidence.

Conclusion

A MIMIM multilayer which formed two FP cavities stacked on top of each other with a common metal layer on a thick Si substrate was the focus of this research and was studied in depth using TMM simulations. It was seen that a FP cavity enhances the response of an optical system to radiation. This MIMIM cavity, as the abbreviated name suggests, was made of alternating dielectric and metal layers on top of a Si substrate.

Initially, three different polarizations were considered and the effect of changing the angle of incidence on the prominent dips in the reflection spectrum of the stack was studied for visible-

infrared region of the electromagnetic spectrum. The amount of reflection, position and depths of the reflection dips varied significantly for all polarizations. It was noted that these reflection minima shifted to lower wavelengths as the angle of incidence was increased in steps between 0 to 80°, for all polarizations, because the component of the wave vector perpendicular to the layer surfaces decreases for a given wavelength.

From these simulations of the effect of change of angle of incidence on the response of the MIMIM structure, it was noted that it is important to stay at lower angle of incidences to get optimum results for all polarizations and this was shown to be a trend for two different stacks (MIMIM TiN Hafnia and MIM Al Hafnia). It was also inferred that the reflection dips in the spectrum of the Al-Hafnia multilayers MIM stack were much narrower and deeper owing to a greater absorption coefficient of Al compared to TiN.

The effects of changing the thickness of each layer was studied, and for the bottom metal layer in the reference MIMIM stack with TiN and Hafnia multilayers, beyond a certain thickness, the response was same. This was also the same in case of the middle metal layer and the first metal layer.

When the thickness of the dielectric layer in the second cavity was changed, the resonant peak in absorption also changed. This was attributed to a change in phase shift of the cavity which changed the resonant wavelength. This was also seen when the dielectric layer in the top FP cavity was changed.

More interesting results were noted for a change of the first metal layer thickness. In the top MIM cavity, if the thickness of the top metal layer is increased to be greater than the thickness of the second metal layer, then there were two prominent absorption peaks. However, for a thicker top metal layer, the other prominent peak fades out and disappears. This was noted as a trend in two MIMIM cavities with different metals (TiN and Al).

This information was extremely useful when designing selective emitters for a TPV system, because only one prominent peak around the bandgap wavelength of the respective converter cell is desired. A thicker top metal layer than the bottom layer in a FP cavity serves the purpose.

It was also cross-checked that the first metal layer thickness must be greater than the dielectric coating thickness to avoid a small peak in the absorption spectrum at low wavelengths.

Simulations were performed for refractive index of TiN and Si from different sources and varying results were obtained. It is best to consider the dependence of n and k on the wavelength for all the materials.

Layer by layer absorption was also studied for the reference MIMIM stack, and the absorption vs depth profile was also calculated and plotted. Another simple FP cavity was studied in this section for better understanding of the amount of absorption in each layer. This data was confirmed to be accurate, because all the absorptions in the layers were added and the total absorption was tallied with that of the original absorption spectrum. For any multilayer, the absorption in the top metal layer is the highest, and decreases in deeper metal layers because there is least electric field penetration into the bottom metal layer.

Density plots of the reflectance, transmittance and absorption of the reference MIMIM stack created using XYZPY package in python were studied for data which had a lot of dimensions. During the design of selective emitters, these plots made it easy to find, predict and optimize the combination of the angle of incidence of the radiation and thickness of each layer to get the desired absorption peaks. It was also confirmed through these density plots that the transmittance in this stack was negligible.

Reference

1. Born, M., Wolf, E. (1999). Principles of optics (7th ed.). Cambridge University Press. https://www.cambridge.org/core/books/principles-of-optics/D12868B8AE26B83D6D3C2193E94FFC32
2. MacLeod, H. A. (2010). Thin-Film Optical Filters (4th ed.). https://kashanu.ac.ir/Files/Content/[H__Angus_Macleod]_Thin-Film_Optical_Filters,_Four(BookFi_org).pdf
3. Yeh, P. (2005). Optical Waves in Layered Media, https://www.wiley.com/en-us/Optical+Waves+in+Layered+Media-p-9780471731924
4. Heavens, O. S. (1991). Optical Properties of Thin Solid Films. https://www.amazon.in/Optical-Properties-Solid-Films-Physics/dp/0486669246
5. Byrnes, S. J. (2016). Multilayer Optical Calculations. GitHub repository. Available: https://github.com/sbyrnes321/tmm.
6. Chubb, D. L. (2007). Fundamentals of Thermophotovoltaic Energy Conversion. https://shop.elsevier.com/books/fundamentals-of-thermophotovoltaic-energy-conversion/chubb/978-0-444-52721-9
7. Yariv, A., & Yeh, P. (2006). Photonics: Optical Electronics in Modern Communications. https://shop.elsevier.com/books/fundamentals-of-thermophotovoltaic-energy-conversion/chubb/978-0-444-52721-9
8. Kim, J. H., Chrostowski, L., Bisaillon, E., & Plant, D. (2007). DBR, Sub-wavelength grating, and Photonic crystal slab Fabry-Perot cavity design using phase analysis by FDTD," Opt. Express 15(16), 10330-10339.
9. (2024). XYZPY Documentation, Available: https://xyzpy.readthedocs.io/en/latest/.
10. I. J. Fritz, J. F. Klem and J. R. Wendt (1991) Reflectance modulator based on tandem Fabry-Perot resonators," Appl. Phys. Lett. 59, 753-755.